Identification of the process of hydromechanical extraction of amber

Zinovii Malanchuk, *Valerii* Korniyenko*, *Yevhenii* Malanchuk, *Andriy* Khrystyuk, and *Mykola* Kozyar

National University of Water Management and Environmental Management, 11 Soborna Str., Rivne, 33028, Ukraine

Abstract. The article deals with the method of hydromechanical extraction of amber from sand deposits. The essence of hydromechanical method of amber extraction is considered. The process of extraction has been identified. The analytical expressions obtained for calculating the parameters of hydromechanical extraction of amber from sand deposits, and in particular the expression for determining the rate of emergence of an amber particle, can be used in the further engineering calculations of process parameters and process equipment. These expressions will allow to accurately substitute and with sufficient accuracy to calculate the parameters of the process of extracting amber from amber-containing deposits, as well as to set the parameters of technological equipment for the implementation of this process.

1 Introduction

The essence of the above method is that the array is saturated with water and activated by mechanical excitation to form a continuous slurry of such density at which there is an ejection force that raises the amber on the surface of the deposit. Mechanical action, when present in an array of water, causes the array to completely lose the bond between the particles, release the amber and reach a suspension state with a density greater than the specific gravity of the amber, which allows the latter to float to the surface of the field at the expense of the field.

To implement the method, it is necessary to dip the rods in the amber array in the form of pipes from which water and air are supplied and on which mechanical exciters are fixed. The array is saturated with water and the working body is oscillated. Amber is released from the environment and floats to the surface [1].

The process of soil liquefaction is as follows. In the amber array vibrating method immerses rods with biconical vibrators while simultaneously feeding water and air into the soil array through them. The array of vibrators is oscillated, thus forming a zone of continuous boiling of the soil. Amber separates itself from the massif and under the action of ejection force floats to the surface. The suspension medium allows the vibration device to move freely in the longitudinal direction.

The use of vibrating gear for the extraction of amber from the fields allows achieving the extraction of amber from the field, increasing labor productivity and reducing energy intensity and negative man-made environmental impact on the environment [2].

To increase production volumes while reducing cost, the industry requires the introduction of advanced technologies in amber production. In the absence of financing in this sector, investments from the state are absent. Amber mining is an outdated method that requires a great deal of money and time to extract and process large amounts of soil to produce amber. Figure 1 shows a diagram of one of the largest amber fields in Ukraine.

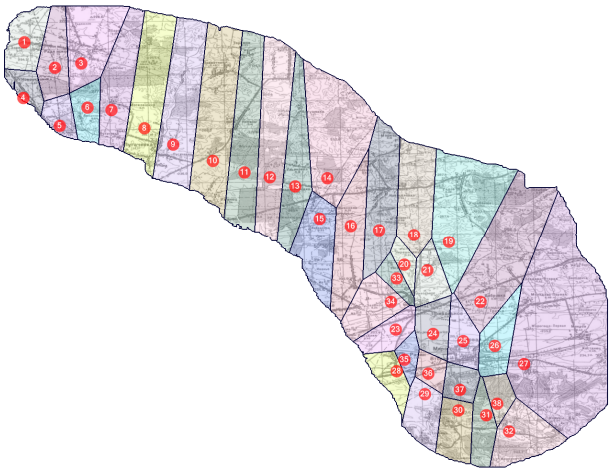

Fig. 1. Klesiv amber deposits.

Thus, today, amber production requires new technologies and the development of means to intensify the extraction process, which achieves high productivity and efficiency, and also reduces the negative environmental impact on the environment [3-9].

2 Methods

The northern regions of the Rivne region are characterized mainly by the occurrence of amber in sandy soils, characterized by water and air pores present

* Corresponding author: kvja@i.ua

© The Authors, published by EDP Sciences. This is an open access article distributed under the terms of the Creative Commons Attribution License 4.0 (http://creativecommons.org/licenses/by/4.0/).

between the soil skeleton. between them, the Sandy soil moves into a mobile state when the equilibrium between the soil skeleton and the water pores is disturbed, and the slight influence of the hydraulic flows can cause the mass to shift and the considerable mass of the soil to a liquefied state. The transition of water-saturated sands to the liquefied state causes destruction of the structure of the sands and their compaction under the influence of their own weight or external influences. When the sand is thinned, the bearing capacity is lost completely or partially, and the fluid state arises as a result of the destruction of the structure and displacement of the sand particles relative to each other, which is accompanied by the formation of a denser particle arrangement and a decrease in porosity.

The liquefaction phenomenon occurs when the structure and possibility of sand compaction are destroyed; full or close to full saturation of sand with water.

In the course of research, the amber sand deposit at the initial stage enters the state of vacuum, and in the subsequent there is its compaction. The duration of water saturated sands in the rarefied state is much shorter than the time of soil compaction. In our opinion, and based on the results of the analysis of literature sources, the compaction process is more investigated than the liquefaction process, so experimental studies of the liquefaction process, the flow of the process of reaching the surface of amber and the time of transition of sandy soil to the compacted state require additional research. In order to create the necessary conditions to reach the surface of the amber, it is necessary to investigate the parameters of vibrational impact and the use of water and air when exposed to a sandy field.

In conducting experimental studies, we studied the environment of amber, while simulating the boiling process and conducted research on the factors and parameters that affect the creation of the suspension environment.

Studies have shown that the liquefaction structure destroys the sandy amber medium. The sand particles, within the vibration range, are separated from the total array and are brought into oscillatory motion near their equilibrium position and are also moved along some trajectory relative to the vibration source. At the same time there is an intensive movement of gas and water, which take with them sand particles and amber and throw them on the surface. Since the surface of the amber significantly exceeds the area of the particles, under the action of Archimedes force pieces of amber are pushed to the surface.

The following stages of transformation are observed during the vibrational action on a sandy soil mass [2]:
- vibration dilution (maximum preparation for intensive mixing);
- vibration boiling (separation of particles and mixing in the array);
- gradual compaction of the sandy soil mass from the periphery to the vibration source.

The effect of the thinning of the layer is similar to the phenomenon of vibration linearization of dry friction, that is, in the presence of vibration to transfer a particle of relative motion in the environment requires less constant force than in its absence. As the effective coefficient of friction decreases in the vibration state, the particles slip away relative to one another. The spreading layer is compacted.

From studies [4-8] it is known that the movement of sand in a vibrating fluid bed is not subject to the law of motion of particles in airless space. In addition to gravity, the trajectory of movement of the sand layer is significantly influenced by the parameters of the environment. Throwing produces a rarefaction, while falling - increasing the pressure of the environment. The lower layers of sandy soil have a greater pressure drop than the upper ones, so the air is displaced from below and seals between the particles.

In this way, the vibrating fluidized bed of sandy soil behaves like a pump that pumps a gas-liquid mixture to the surface, taking particles of amber and transporting them to the top. In this case, the rate of rise of the particle from bottom to top depends on the vibrational excitation of the array, the dilution of the medium, saturation with air bubbles and the viscosity of the medium.

The pressure drop depends on the frequency and amplitude of the oscillator, the height of the layer, the particle size and humidity of the sandy soil, as well as the coefficient of friction of the particles one by one. The intensity of the pumping action of the vibrating boiling layer is characterized by three parameters: pressure above and rarefaction under the vibrating boiling layer, pressure drop in the layer.

The following parameters influence the creation of a vibrating fluid layer of soil: 1) oscillation amplitude; 2) oscillation frequency; 3) compelling force; 4) water pressure; 5) air pressure; 6) geometric arrangement of the oscillators.

To a large extent, these parameters are experimentally determined.

Submission into the sand mass of air together with water can intensify the process of lifting the amber to maximum values, but when the air trunks are formed, the boiling process goes into vibration and stops. The maximum rate of flow of amber to the day surface is observed when changing the flow of gas-liquid mixture in the sand array in the range 0 to 0,02 m^3/h.

Creating the desired density of the medium depends on the flow of gas-liquid mixture into the array.

Figure 2 shows the results of experimental studies of the simultaneous influence of the oscillation frequency of the working body and the magnitude of the air flow into the sand array, which demonstrate the explicit manifestation of two peak areas of maximum amber flow velocities [10].

On the basis of the obtained experimental dependence, we have the following ranges of values of the oscillation frequency of the working body and the magnitude of the air flow into the amber-containing array: the oscillation frequency of the working body 28-34 Hz; the magnitude of the air flow into the array 0,003-0,006 m^3/h, with the speed of lifting amber is the highest and is 0,09-0,12 m/s [10].

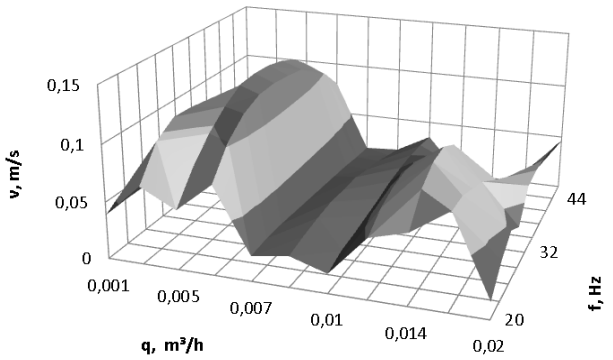

Fig. 2. Dependence of the amber rise rate on the frequency of oscillation and the supply of air to the water-saturated array.

3 Results and discussion

3.1 Analysis of models of motion of an amber particle under hydromechanical action

The movement of amber in a sandy massif is characterized by movement with resistance to the type of dry friction. The movement of a particle placed in a medium that performs horizontal oscillations with frequency and radius of the trajectory and produces a particle resistance similar to dry friction. The corresponding problem was considered by V. V. Gortinsky, G. E. Ptushkin and I. I. Blechmann [11]. Here are the main results of the solution and their discussion in terms of hydromechanical amber production. These authors have considered the following system of differential equations of motion of a particle with respect to the medium to determine the rate of emergence of amber

$$m_1\ddot{x} = m_0(\Delta - 1)rf^2\cos ft - F_h\frac{\dot{x}}{\sqrt{\dot{x}^2+\dot{y}^2+\dot{z}^2}}, \quad (1)$$

$$m_1\ddot{y} = m_0(\Delta - 1)rf^2\cos ft - F_h\frac{\dot{y}}{\sqrt{\dot{x}^2+\dot{y}^2+\dot{z}^2}}, \quad (2)$$

$$m_1\ddot{z} = m_0(\Delta - 1)g - F_v\frac{\dot{z}}{\sqrt{\dot{x}^2+\dot{y}^2+\dot{z}^2}}, \quad (3)$$

$$\Delta = \rho / \rho_0, \quad (4)$$

$$\sqrt{\dot{x}^2+\dot{y}^2+\dot{z}^2} \neq 0. \quad (5)$$

where F_v – the force of resistance to the relative displacement of the particle in the vertical direction, N;
m_1 – the mass of the particle taking into account the attached mass of the medium, kg;
m_0 – mass of the medium in volume equal to the volume of the particle, kg;
$\dot{x}, \dot{y}, \dot{z}$ – projections on the axis of the rectangular coordinate system XYZ of the relative velocity of the particle in the medium, m.

This allowed them to propose the following dependence for determining the rate of emergence of amber [12]:

$$v = \frac{a^2}{\sqrt{\left(\frac{F}{gm}\right)^2 - a^2}}\frac{\alpha}{k_m}, \quad (6)$$

$$\alpha = \begin{cases} Af, & A^2 f < kg \\ \frac{kg}{f}, & A^2 f > kg \end{cases}, \quad (7)$$

$$a = \rho - 1, \quad (8)$$

$$\rho = \frac{\rho_c}{\rho_s}, \quad (9)$$

where v – the rate of emergence of the amber particles, m/s;
m – weight of amber particles, kg;
a – the Archimedes parameter for the amber particle;
g – free fall acceleration, m/s^2;
k_m – the coefficient of the coupled mass;
f – frequency of oscillation of the working body, Hz;
F – the force of resistance of the sand layer relative to the motion of the amber particle [12];
ρ_s – density of amber particles, kg/m^3;
ρ_c – density of water-sandy environment, kg/m^3;
A – oscillation amplitude of the working body, m;
k – coefficient of friction.

Formula (6) is obtained for the case of particle flooding of lower density in the layer of particles of heavier material when the oscillation of the working body in the plane of the surrounding medium [13-17]. In this case, the authors assume that apart from the forces of inertia, Archimedes, and gravity, only the forces of resistance to relative motion are active, and the trajectory of motion of the particle is a spiral.

However, there are no recommendations for determining the magnitude of the force for the conditions under consideration. Given the dimension and nature of this magnitude, as well as the fact that it characterizes the interaction between the amber particle and the soil skeletal particles, the following option is proposed to determine the magnitude of this force

$$\frac{F}{gm} = \phi(1+a), \quad (10)$$

where ϕ – the drag coefficient of the sand medium of the amber particle motion [18].

Substituting the dependence (10) into formula (6), the following expression is obtained for the rate of emergence of an amber particle:

$$\frac{k_m v}{\alpha} = \frac{a^2}{\sqrt{\phi^2(1+a)^2 - a^2}}. \quad (11)$$

The obtained formula (11) takes into account the influence of the difference in the density of the soil particles and the extracted material, as well as the amplitude and frequency of oscillation of the working body. The effect of the air supply is only taken into account by changing the density of the amber-containing medium.

To determine the magnitude of the coefficient ϕ we will use the results of experimental studies by well-known authors on the emergence of amber particles in laboratory and field conditions [19-29]. In this case, expression (11) will have a more convenient definition for ϕ:

$$\varphi = \sqrt{1+\frac{\alpha}{k_m v}}\left(1-\frac{\rho_s}{\rho_c}\right). \quad (12)$$

From the received data it is visible that for the whole interval of the studied values at calculations with engineering accuracy it is possible to use the average value of the coefficient ϕ equal to

$$\phi = 0{,}325. \quad (13)$$

It follows from formulas (6) - (13) that in hydromechanical extraction of amber from sand deposits, the ratio of the force that impedes the movement of the particle in the bulk medium to the volume of the particle, the density of the medium and the acceleration of free fall is equal to 0,325.

The results of the study of expression (11) on the extreme indicate that this function has a maximum at a point:

$$a_{\max} = \frac{3}{2}\frac{\phi^2}{1-\phi^2}\left[1+\sqrt{1+\frac{8}{9}\frac{1-\phi^2}{\phi^2}}\right], \quad (14)$$

the coordinate of which at $\phi = 0{,}325$ is $a_{\max} = 0{,}6946$.

Thus, it is necessary to consider the motion of the amber particle in the vertical direction, taking into account Archimedes force, vibrations of the working body, as well as the forces of relative resistance of the medium and viscous friction [30-36]. In this case, given the results already obtained and the assumption that the positive direction of the coordinate axis is directed vertically upwards, the equation of motion of the floating particles can be written as follows:

$$\left(1+k_m\right)m\frac{d^2z}{dt^2} = m_0 ga + m_0 Sf^2 \sin ft - F - F_c, \quad (15)$$

$$m = \rho_s \frac{\pi d^3}{6}, \quad (16)$$

$$m_0 = \frac{\rho_c}{\rho_s} m, \quad (17)$$

$$F = \phi m_0 ga, \quad (18)$$

$$F_c = C_x \rho_c \frac{v^2}{2}\frac{\pi d^2}{4}, \quad (19)$$

where z – moving particles of amber, m;
t – time, s;
m_0 – weight of amber-containing sand in the volume of amber particles, kg;
S – the oscillation amplitude of the working body, m;
F_c – the force of viscous friction of an amber particle when moving through a liquefied medium, N;
d – diameter of amber particles, m;
C_x – force coefficient of viscous resistance.

Taking into account recommendations [37-49], we assume that the Stokes regime of the flow of amber particles when moving through a liquefied fluidized medium, for which according to [29] the dependence of the coefficient of viscous drag force on the Reynolds number can be distinguished as follows:

$$C_x = \frac{26}{\mathrm{Re}_c}, \quad (20)$$

$$\mathrm{Re}_c = \frac{vd}{\nu_c}, \quad (21)$$

where Re_c – Reynolds number characterizing the process of interaction of the amber particle with the liquefied medium;
ν_c – kinematic viscosity of the liquefied medium.

Substituting formulas (16) - (21) into equation (15) and having the corresponding transformations, we obtain the following equation of motion of an amber particle through a liquefied medium

$$\frac{d^2\zeta}{d\tau^2} + f_0^2\frac{d\zeta}{d\tau} = A_0\frac{\rho-1}{\rho} + A\sin a\tau, \quad (22)$$

$$\zeta = \frac{z}{d}, \quad (23)$$

$$\tau = \frac{gd}{\nu_g}t, \quad (24)$$

$$f_0 = \sqrt{\frac{39\sigma}{2\left(1+k_m\right)\rho Gm}}, \quad (25)$$

$$A_0 = \frac{\left(1-f\right)}{\left(1+k_m\right)\rho Gm}, \quad (26)$$

$$A = \frac{a^2}{\left(1+k_m\right)\rho}\frac{S}{d}, \quad (27)$$

$$a = \frac{\omega\nu_g}{gd}, \quad (28)$$

$$Gm = \frac{gd^3}{\nu_g^2}, \quad (29)$$

$$\sigma = \frac{\nu_c}{\nu_g}, \quad (30)$$

$$\rho = \frac{\rho_c}{\rho_s}, \quad (31)$$

where σ – the viscosity ratio of the liquefied medium [10];
ρ – the relative density of the liquefied medium;
ν_g – kinematic coefficient of air viscosity.

The solution of equation (22) is investigated and reported in the specialized literature, and it is proved that the periodic term, when averaging, makes no significant

contribution compared to the stationary component [15]. Thus, the amber medium can be considered as a liquefied layer when the hydromechanical action disrupts the contact between the amber particles and the particles of the array, between the particles of the amber-containing array, but does not directly affect the movement of the amber particles. The effect is to increase the mobility of the particles and the porosity of the array, to reduce the friction between the particles, as well as to obtain an array of viscosities similar to the kinematic viscosity of a liquid substance [29]. That is, the hydromechanical effect creates favorable conditions for the work of Archimedes force, which ensures that the particles of amber float to the surface.

In this case, the equation of motion of the amber particle with hydromechanical action on the amber-containing layer takes the following form

$$v = \frac{2(1-f)}{39}\frac{gd^2}{\sigma\nu_g}\frac{\rho-1}{\rho}. \quad (32)$$

Given the ratio of the density of the flooded soil to the air, the relative density of the liquefied medium can be determined by the following formula:

$$\rho = (1-\varepsilon)\Delta, \quad (33)$$

$$\Delta = \frac{\rho_0}{\rho_s}, \quad (34)$$

where ε – the porosity of the liquefied medium;
Δ – the ratio of the particle densities of the water-saturated soil to the soil and amber.

The results of experimental studies on the measurement of the density of a layer of water-saturated soil containing particles of amber under hydromechanical exposure with and without air supply show that the porosity of the medium under the considered influence on the soil mass with engineering accuracy can be determined.

At the same time, formulas (32) - (34) should describe the dependence of the flow rate of the amber particles on the air flow, with a characteristic maximum in the neighborhood of q = 0,015 m^3/h. Substituting expression (33) into formula (32), it is easy to obtain an expression for the first derivative of q:

$$\frac{dv}{dq} = -\frac{\beta+2\alpha q}{(1-\varepsilon)^2}\frac{2(1-f)}{39\Delta\sigma}\varepsilon_\omega\frac{gd^2}{\nu_g}. \quad (35)$$

It can be seen from formula (35) that the dependence (32) on the variable q is decreasing over the entire interval and has no extremes. This means that in order to adequately describe the processes under consideration, it is necessary to take into account the change in not only the density but also the effective viscosity of the liquefied medium. Similar processes are realized in the processing of bulk material in vibrating, boiling and pulsating fluidized layers [12-24]. The results of the analysis of known mathematical models describing hydrodynamic processes in such layers with steady or pulsed air supply suggest two types of formulas for calculating the dynamic viscosity coefficient of the liquid medium under consideration [29].

The first group of formulas, to which Einstein's dependencies [15], Vakhrushev, Gupalo, Kunitz, and Todesa [29] include, depend on the degree of porosity without taking into account the influence of other factors:

$$\sigma = \frac{M}{\varepsilon^N}. \quad (36)$$

However, the authors do not indicate what determines the values of the coefficients in formula (36), how to choose them, and how to consider other factors, such as the volume air flow, the size and density of soil particles. The formulas of the second group [15] take these factors more fully into account, which complicates the calculated dependencies and requires their adaptation to the conditions of use.

The maximum effect of these parameters is taken into account in determining the dynamic viscosity of the liquefied medium by the following method [29]:

$$\mu = 0,7282\frac{g^{1,207}\delta^{2,207}\rho_g^{0,707}}{(v_g-v_0)^{1,414}}\rho_0^{0,293}\sqrt{1-\varepsilon}, \quad (37)$$

$$v_0 = \frac{v_g}{4,9}\left(\frac{\rho_0}{\rho_g}\right)^{0,1}, \quad (38)$$

where μ – the dynamic viscosity of the liquefied medium;
δ – diameter of particles of soil skeleton containing amber, m;
ρ_g – air density, kg/m^3;
ρ_0 – density of water saturated amber medium, kg/m^3;
v_g – air speed, m/s;
v_0 – the sliding velocity of particles of amber-containing medium, m/s.

Substituting expression (37) into formula (38), moving from a dynamic coefficient of viscosity to a kinematic coefficient of viscosity, conducting the corresponding transformations and transition to dimensionless quantities, taking into account formula (34), after approximating the dependence of the coefficient of proportionality on the ratio of the density ratio and air by a power function, we obtain the following expression for calculating the magnitude σ:

$$\sigma = k_v\frac{Gm^{1,207}}{\rho\,\mathrm{Re}_g^{1,414}}\sqrt{1-\varepsilon}, \quad (39)$$

$$k_v = 0,6898\Delta^{0,407}\left(\frac{\rho_g}{\rho_s}\right)^{0,593}, \quad (40)$$

$$\mathrm{Re}_g = \frac{v_g\delta}{\nu_g}, \quad (41)$$

$$Gm = \frac{g\delta^3}{\nu_g^2}, \quad (42)$$

where Re_g – Reynolds number characterizing the process of interaction of the particles of the liquefied medium with the incoming air;
Gm – dimensionless complex.

The Reynolds number characterizing the process of formula (44) includes the characteristic air velocity, for which it is recommended to use the following dependences when considering the processes occurring in the layer [15]:

$$\tilde{q} = v_g F_g \varepsilon_u , \quad (43)$$

$$\varepsilon_u = 1,2\varepsilon_* \left(\frac{v}{v_*} \right)^{\theta} , \quad (44)$$

$$\theta = 0,08 + 4 \cdot 10^{-8} a_0 Gm , \quad (45)$$

$$a_0 = \frac{\rho_0 - \rho_g}{\rho_g} , \quad (46)$$

where $\tilde{q}$ – volume flow rate of air supplied to the soil, m^3/s;
F_g – the characteristic area on which the air from the nozzle head liquefies the soil layer, m^2;
ε_u – effective porosity of the soil layer;
ε_* – effective porosity of the soil layer at the initial moment of liquefaction;
v_* – air velocity, providing the beginning of liquefaction, m/s;
θ – exponent;
a_0 – the Archimedes parameter for an amber-containing soil particle in the air supply.

The results of the calculations performed by the formula (45) show that the values of the density and particle size of the skeleton of the sandy-clay mixture under study, without losing the accuracy of the value of the exponent θ can be considered equal 0,08.

Based on this, using the results of experimental studies on the measurement of the density of the soil layer containing particles of amber under hydromechanical action with and without air supply, the dependence (44) can be rewritten as follows:

$$\varepsilon_u = \varepsilon_\omega \left(\frac{\tilde{q}}{\tilde{q}_\omega} \right)^{0,08} , \quad (47)$$

where $\tilde{q}_\omega$ – characteristic air supply, $\tilde{q}_\omega = 0,000217$.

To estimate the characteristic area on which the air from the nozzle head liquefies the soil layer, we will use recommendations for choosing the geometric parameters of the probe used for direct impact on the soil, in particular, the estimate of the distance between adjacent rods [10, 15, 24, 29]. Assuming that the air exiting the nozzle liquefies the soil to a volume limited by two axial cylinders. The outer cylinder radius is equal to this value and the inner cylinder radius is equal to the radius of the bar. In this case, the value F_g can be determined from the following formula [15]:

$$F_g = \pi tg\phi \left(\frac{d_T}{h_{dd}} + tg\phi \right) h_{dd}^2 , \quad (48)$$

where ϕ – the taper angle of the nozzle through which air is supplied;
d_T – the diameter of the bar on which the attachment is attached, m;
h_{dd} – length of the conical part of the working body, m.

Substituting formulas (44) - (48) into expression (43), after performing all the transformations taking into account (39) - (43), we obtain the following dependencies for determining the value σ:

$$\sigma = k_\sigma \frac{\sqrt{1-\varepsilon}}{\rho z^{1,3}} , \quad (49)$$

$$k_\sigma = K \left(\frac{\rho_g}{\rho_s} \right)^{0,593} Gm^{0,735} \Delta^{0,407} \frac{\varepsilon_\omega^{1,414}}{1,45} , \quad (50)$$

$$K = \left(\frac{\sqrt[3]{g v_g} h_{dd}^2}{1,37 \tilde{q}_\omega} \right)^{1,414} , \quad (51)$$

$$z = \frac{\tilde{q}}{\tilde{q}_\omega} , \quad (52)$$

where *K* – dimensionless technological constant;
z – dimensionless air flow.

Thus, a joint consideration of formulas (32) - (34), (10), (11) and (49) - (52) gives us the following dependencies for determining the rate of emergence of an amber particle under hydromechanical action on a water-sandy massif:

$$\mathrm{Re} = \frac{w}{\Delta^{0,407} \varepsilon_\omega^{1,414}} \frac{(1-\varepsilon)\Delta - 1}{\sqrt{1-\varepsilon}} z^{1,3} , \quad (53)$$

$$\mathrm{Re} = \frac{vd}{v_g} , \quad (54)$$

$$w = \frac{1-f}{13,45K} \left(\frac{\rho_s}{\rho_g} \right)^{0,593} \left(\frac{d}{\delta} \right)^3 Gm^{0,265} , \quad (55)$$

where Re – Reynolds number, which characterizes the process of the emergence of amber particles through a vibrating pneumatic fluid medium.

It is convenient to rewrite the right part of expression (53) in the following form, bringing the two terms in the numerator and denominator to the same form

$$\frac{\mathrm{Re}}{W} = \frac{1 - n\varepsilon}{\sqrt{1-\varepsilon}} z^{1,3} , \quad (56)$$

$$W = w \frac{\Delta - 1}{2,2\Delta^{0,407} \varepsilon_\omega^{1,414}} , \quad (57)$$

$$n = \frac{\Delta}{\Delta - 1} . \quad (58)$$

Given that the value of soil porosity in hydromechanical impact is subject to the following restriction from above

$$\varepsilon < 1 , \quad (59)$$

then, based on the rules of representation of functions of this kind in power series, the dependence (56) can be rewritten as follows (Fig. 3): then, based on the rules of representation of functions of this kind in power series, the dependence (56) can be rewritten as follows (Fig. 3):

$$U = \left(1 - \left[\gamma + \beta z + \alpha z^2\right]\varepsilon_\omega\right)^m z^{1,3}, \qquad (60)$$

$$U = \frac{\mathrm{Re}}{W}, \qquad (61)$$

$$m = \frac{1}{2}\frac{\Delta+1}{\Delta-1}. \qquad (62)$$

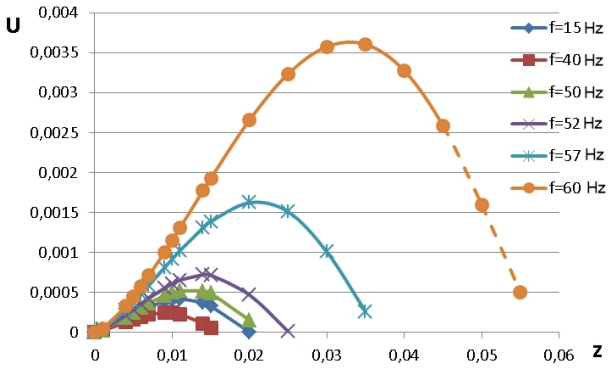

Fig. 3. Dependency graphs *U* from dimensionless air flow at different oscillations of the working body.

From Fig. 3 it is seen that the obtained dependence of the dimensionless velocity of the particles of amber on the dimensionless flow rate (60) has a maximum in the range of values of air flow close to the experimentally obtained value, in the vicinity q = 0,015 m^3/h, which depends on the frequency of oscillation of the working body, similar to the results obtained in laboratory and field experiments [29].

Comparison of the results of the formulas (60) made for the frequency of 30 Hz with the results of experimental laboratory studies shows a satisfactory coincidence of the results of the calculations and experiments in the area q = 0,015 m^3/h (Figs. 4, 5). Thus, in the volume flow rate range from 0,014 to 0,025 m^3/h, the relative error of calculations does not exceed 10%.

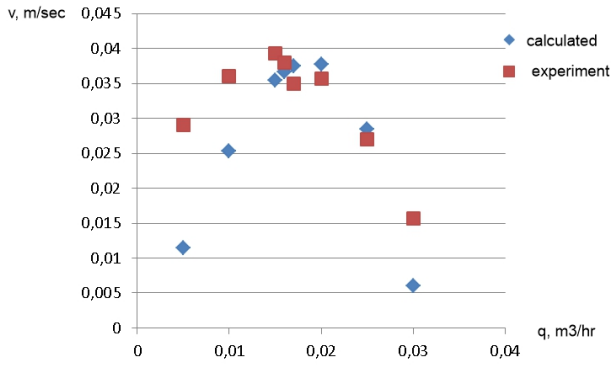

Fig. 4. Dependence of the amber particle floating rate on the air volume supplied at a 30 Hz oscillator.

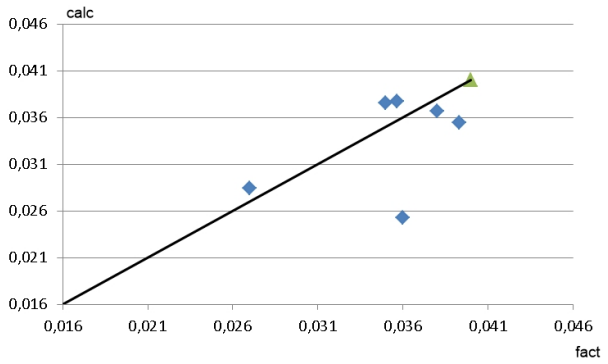

Fig. 5. Comparison of the results of calculations and experiments at the oscillation frequency of the working body of 30 Hz (error of calculations does not exceed 10%).

3.2 Determination of the rational parameters of the process of hydromechanical extraction of amber from sand deposits

The study of the dependence (60) on the extreme, by approximating the first derivative in magnitude to zero, indicates the existence of a maximum of the function under study at the following value of dimensionless air flow:

$$z_{\max} = \sqrt{A^2\left(\frac{\beta}{2\alpha}\right)^2 + B\frac{1-\varepsilon_\omega\gamma}{\varepsilon_\omega\alpha}} - A\frac{\beta}{2\alpha}, \qquad (63)$$

$$A = \frac{1{,}3\Delta - 0{,}8}{2{,}3\Delta - 0{,}3}, \qquad (64)$$

$$B = \frac{1{,}3(\Delta-1)}{2{,}3\Delta - 0{,}3}, \qquad (65)$$

where $z_{\max}$ is the value of dimensionless air flow at which the maximum velocity of the particles of amber is realized.

Substituting expression (63) into formula (60) and performing the corresponding transformations and erections of such terms, we obtain the following dependence for determining the maximum rate of emergence of amber particles under hydromechanical action on the water-sandy massif:

$$\mathrm{Re}_{\max} = W_\Delta\left(z_\omega - z_{\max}\right)^m z_{\max}^{1,3}, \qquad (66)$$

$$z_\omega = \frac{1-\gamma\varepsilon_\omega}{\varepsilon_\omega\beta}\frac{\Delta+1}{\Delta+0{,}5}, \qquad (67)$$

$$W_\Delta = w\frac{\Delta-1}{\Delta^{0{,}407}}\left(\frac{\Delta+0{,}5}{2{,}3\Delta-0{,}3}\right)^m \varepsilon_\omega^{m-1{,}414}\beta^m. \qquad (68)$$

Comparison of the results of formulas (63) and (66) performed for the frequency of 30 Hz with the results of experimental laboratory studies shows sufficient accuracy for engineering calculations and: relative error for air flow does not exceed 11,3% (calculation – 0,0133 and fact – 0,015 m^3/year); and for the maximum velocity of the particles of amber is 32,5% (the calculation is 0,053 and the fact is 0,04 m/s). The high error in

determining the maximum floating velocity can be explained by the significant dependence of this value on the particle size of the amber and the skeleton of the water-saturated soil, which varied during the experimental studies at fairly wide intervals.

Comparison of the results of the calculations according to formula (63) with the results of other authors [2-9, 15, 17-29] (Figs. 6, 7) confirms the reliability of the proposed dependence obtained for laboratory studies at a frequency of 30 Hz (Fig. 8, 9).

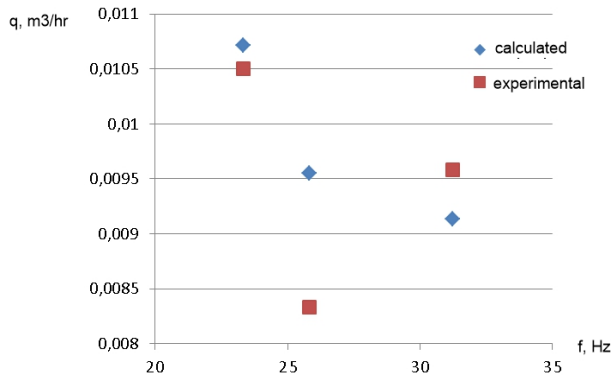

Fig. 6. The dependence of the air flow rate, which provides the maximum flow rate of the amber particles obtained by calculation (63) and according to experiments, from the frequency of oscillation of the working body.

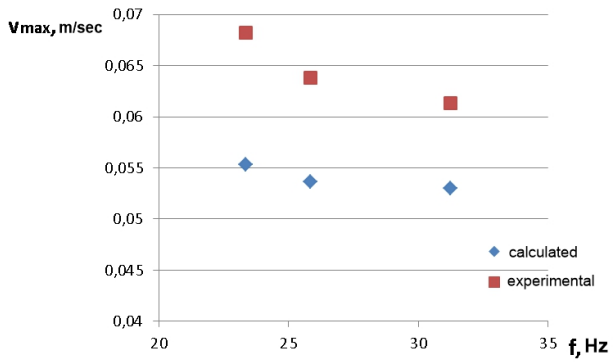

Fig. 7. The dependence of the maximum rate of emergence of amber particles obtained by calculation (63) and according to experiments, on the frequency of oscillation of the working body.

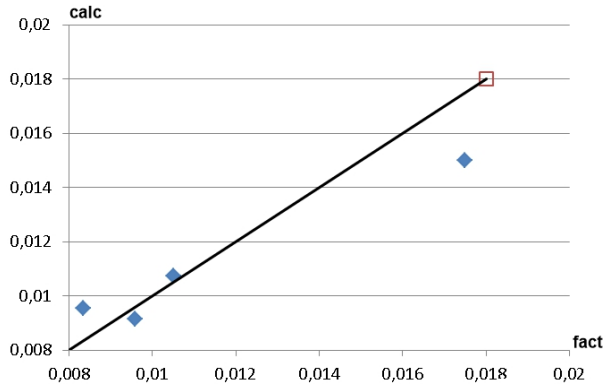

Fig. 8. Comparison of the results of the calculations by (63) and the experiments to determine the air flow rate, which provides the maximum velocity of amber particles (relative error does not exceed 11,3%).

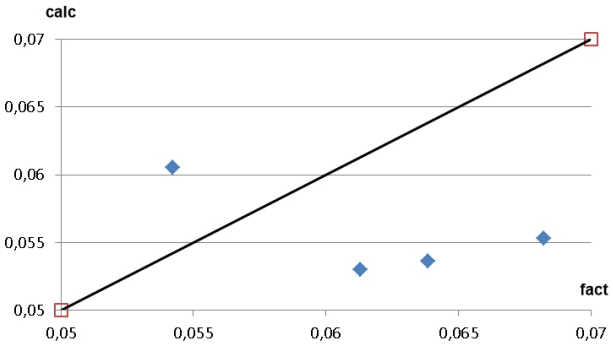

Fig. 9. Comparison of the results of the calculations for (63) and experiments to determine the maximum rate of emergence of amber particles.

The results of the numerical analysis of the terms on the right-hand side of formula (63) indicate that it is possible to use for engineering calculations the air flow rate, which provides the maximum velocity of the particles of amber, the following simplified dependence:

$$z_{\max} = 0,008\frac{\Delta^{0,281}}{\sqrt{\varepsilon_\omega}}. \qquad (69)$$

Joint consideration of formulas (66) - (69), with preliminary approximation of complexes depending on the value Δ degree functions, allows you to propose the following simplified dependence for engineering calculations of the maximum velocity of the particles of amber floating:

$$\mathrm{Re}_{\max} = \frac{w\gamma^m}{500}\frac{\Delta^{1,86}}{\varepsilon_\omega^{2,064}}. \qquad (70)$$

Conclusions

Studies have shown that the maximum possible rate of emergence of amber in hydromechanical extraction of sand deposits is directly proportional to the square of the diameter of the particles of amber and the medium, and inversely proportional to the square of the porosity of the soil, which arises from the oscillation of the working organ 20 to 35 Hz without air supply, and its dependence on the density ratio of the soil particles and the material extracted is described by a power function with a positive fractional index of 1,86.

The analytical results obtained confirm the experimental data quite accurately, which allows us to use them in the future for engineering calculations. The obtained expressions will allow with sufficient accuracy to calculate the parameters of the process of extracting amber from amber-containing deposits, as well as to set the parameters of technological equipment for the implementation of this process.

References

1. A. Malka, Historical amber mine at the Amber Mount, in *Conference: ProGEO WG3 meeting 2010. International Conference on Geodiversity, natural and cultural heritage of the Kaszuby Region*

(Eastern Pomerania – Poland). Guide-Book of the field excursion, 6 – 10 September 2010, Gdańsk, Poland

2. M. Krinitskaya, V. Nesterovsky, Influence of the behavior of the pre-cenozoic surface of takarst processes on the formation of amber deposits in the Rivne Polesie. Collection of scientific papers of the Institute of geological Sciences of the national Academy of Sciences of Ukraine 3, 271–275 (2010)
3. I.D. Van der Werf, D. Fico, G.E. De Benedetto, L. Sabbatini, The molecular composition of Sicilian amber. Microchemical Journal **125**, 85–96 (2016). doi:10.1016/j.microc.2015.11.012
4. V.I. Alekseev, The beetles (Insecta Coleoptera) of Baltic amber: the checklist of described species and preliminary analysis of biodiversity. Zoology and Ecology, **23(1)**, 5–12 (2013). doi;10.1080/21658005.2013.769717
5. D. Antoljak, D. Kuhinek, T. Korman, T. Kujundzic, Dependency of specific energy of rock cutting on specific drilling energy. Rudarsko Geolosko Naftni Zbornik **33(3)**, 23–32 (2018). doi:10.17794/rgn.2018.3.3
6. O. Belichenko, J. Ladzhun, Complex gemological research of new types of treated amber. Visnyk of Taras Shevchenko National University of Kyiv. Geology **4(75)**, 30–34 (2016). doi:10.17721/1728-2713.75.04
7. A. Krek, M. Ulyanova, S. Koschavets, Influence of land-based Kaliningrad (Primorsky) amber mining on coastal zone. Marine Pollution Bulletin **131**, 1–9 (2018). doi:10.1016/j.marpolbul.2018.03.042
8. J. Poulin, K. Helwig, The characterization of amber from deposit sites in western and northern Canada. Journal of Archaeological Science: Reports **7**, 155–168 (2016). doi:10.1016/j.jasrep.2016.03.037
9. Q.Y. Xing et al. Study on the Gemological Characteristics of Amber from Myanmar and Chinese Fushun, Key Engineering Materials, **544** (2013). doi:10.4028/www.scientific.net/KEM.544.172
10. Y. Malanchuk, V. Korniienko, V. Moshynskyi, V. Soroka, A. Khrystyuk, Z. Malanchuk, Regularities of hydromechanical amber extraction from sandy deposits. Mining of Mineral Deposits 13(1), 49–57 (2019). doi:10.33271/mining13.01.049
11. V. Poturaev, A. Voloshin, V. Ponomarev, One-dimensional flow of a two-phase medium. Soviet Applied Mechanics 25(8), 843–850 (1989)
12. M. Krinitskaya, V. Nesterovsky, Paleocarst declines as promising traps of amber deposits within the North-Western slope of the mountain, in *Abstracts of the Second International scientific and practical conference "Ukrainian amber world"*, 2008, p. 31
13. A. Malka, R. Kramarska, The mining of Baltic amber deposits in Poland, in *The intonational amber researcher symposium*, Gdańsk, Poland, 2013
14. A. Kumar, Z. Wang, S. Ni, C. Li, Amber: a debuggable dataflow system based on the actor model. Proceedings of the VLDB Endowment **13**(5), 740–753 (2020). doi:10.14778/3377369.3377381
15. Z. Malanchuk, V. Moshynskyi, Y. Malanchuk, V. Korniienko, Physico-Mechanical and Chemical Characteristics of Amber. Non-Traditional Technologies in the Mining Industry. Trans Tech Publications Inc. Solid State Phenomena, **277** (2018). doi:10.4028/www.scientific.net/SSP.277
16. A.M. Zakharenko, K.S. Golokhvast, Using Confocal Laser Scanning Microscopy to Study Fossil Inclusion in Baltic Amber, a New Approach. Key Engineering Materials **806** (2019). doi:10.4028/www.scientific.net/KEM.806.192
17. K. Karmanov, B. Burnashov, B. Chubarenko, Contemporary Dynamics of the Sea Shore of Kaliningrad Oblast. Archives of Hydro-Engineering and Environmental Mechanics **65**(2), 143–159 (2018). doi:10.1515/heem-2018-0010
18. D. Chen, Q. Zeng, Y. Yuan, W. Luo, Baltic amber or Burmese amber: FTIR studies on amber artifacts of Eastern Han Dynasty unearthed from Nanyang. Spectrochimica Acta Part A Molecular and Biomolecular Spectroscopy **222**, 117270 (2019). doi:10.1016/j.saa.2019.117270
19. S. Paynter, M.C. Jackson, Mellow yellow: An experiment in amber. Journal of Archaeological Science: Reports **22**, 568–576 (2018). doi:10.1016/j.jasrep.2017.11.038
20. B. Radwanek-Bąk, M. Nieć, Valorization of undeveloped industrial rock deposits in Poland. Resources Policy **45**, 290–298 (2015). doi:10.1016/j.resourpol.2015.07.001
21. L.J. Seyfullah, E.M. Sadowski, A.R. Schmidt, Species-level determination of closely related araucarian resins using FTIR spectroscopy and its implications for the provenance of New Zealand amber. PeerJ **3**, e1067 (2015). doi:10.7717/peerj.1067
22. A. Mitchell, Hukawng Basin, the Amber Mines, and the Orbitolina Limestone. Geological Belts, Plate Boundaries, and Mineral Deposits in Myanmar, 524 (2018). doi:10.1016/B978-0-12-803382-1.00013-4
23. Y. Wang, Y. Li, F. Liu, Q. Chen, Characteristics of Hydrothermally Treated Beeswax Amber. Gems and Gemology **55**(3) (2019). doi:10.5741/GEMS.55.3.370
24. Y. Malanchuk, V. Moshynskyi, V. Korniienko, Z. Malanchuk, Modeling the process of hydromechanical amber extraction. E3S Web Conf. **60** (2018). doi:10.1051/e3sconf/20186000005
25. R. Cruickshank, Geology of an amber locality in the Hukawng Valley, northern Myanmar. Journal of Asian Earth Sciences **21**(5), 441–455 (2003)
26. M. Lustyuk,Physical and technical bases of hydraulic extraction of lumpy materials from placer deposits. Exactly: Europe 234 (2005)

27. M. Lustyuk, Fundamentals of mechanical and hydraulic mining. Scientific Bulletin of NSU 3, 33–36 (2007)
28. V.M. Matsui, U.Z. Naumenko, O.L. Aleksandrov, G.O. Kuzmanenko, Problems of the amber polesia of ukraine related to the development of amber-succinite deposits. Visnyk Nacionalnoyi Akademiyi Nauk Ukrainy 11, 45–52 (2019). doi:10.15407/visn2019.11.045
29. Z. Malanchuk, V. Korniienko, Y. Malanchuk, Results of research into amber mining by hydromechanical method. Mining of Mineral Deposits **11**(1), 93–99 (2017). doi:10.15407/mining11.01.093
30. I. Sadovenko, M. Lustyuk, *Theoretical and applied bases of mechanical and hydraulic technology of testing, design and development of amber deposits in Ukraine* (Publishing house of the European University, Kyiv, 2008)
31. V.M. Masley, D.K. Mozgovoy, K.G. Bilousov, V.S. Horoshilov, O.S. Bushanska, N.G. Galich, Methods of the impact evaluation of amber mining by multispectral satellite images. Kosmicna Nauka i Tehnologia **22**(6), 26–36 (2016). doi:10.15407/knit2016.06.026
32. M. Lustyuk, Classification of systems for testing and development of amber deposits. Mining, construction, road and land reclamation machines 69, 34–41 (2007)
33. X. Li, L. Huang, J. Zhou, G. Zhao, Review and prospect of mining technology in hard rock mines. Chinese Journal of Nonferrous Metals **29**(9), 1–20 (2019). doi:10.19476/j.ysxb.1004.0609.2019.09.04
34. J. Keenan, D. Kemp, J. Owen, Corporate responsibility and the social risk of new mining technologies. Corporate Social Responsibility and Environmental Management **26**(2) (2019). doi:10.1002/csr.1717
35. K. Szamalek, Amber as a strategic raw material. Biuletyn - Panstwowego Instytutu Geologicznego 466 (2016). doi:10.5604/01.3001.0009.4326
36. A.O. Kyselov, Combating illegal amber mining: Peculiarities of conflict resolution. Naukovyi Visnyk Natsionalnoho Hirnychoho Universytetu 2, 146–152 (2019). doi:10.29202/nvngu/20192/19
37. M. Lustyuk, Description of the technological scheme for the development of amber deposits. Vestnik NUVGP 2 (34), 214–220 (2006)
38. V. Arens, *Fundamentals of the methodology of mining science* (2001)
39. S. Gumenik, A. Sokil, E. Semenenko, V. Shurygin, Problems of development of placer deposits. Sich 224 (2001)
40. N. Shvaher, T. Komisarenko, S. Chukharev, S. Panova, Annual production enhancement at deep mining. E3S Web of Conferences **123**, 01043 (2019)
41. A. Abramov, *Processing, enrichment and complex use of solid minerals* (Moscow state mining University Press, Moscow, 2001)
42. O. Romanovsky, V. Kirikovich, Research of flotation properties of amber. Vestnik UDUWGP 2(26), 323–328 (2004)
43. Yu. Baranov, B. Bluess, E. Semenenko, V. Shurygin, *Justification of parameters and modes of operation of hydrotransport systems of mining enterprises* (National Academy of Sciences of Ukraine, Institute of geotechnical mechanics, Kyiv, 2006)
44. V. Poturaev, A. Bulat, A. Voloshin, S. Ponomarenko. *Mechanics of vibration-pneumatic ejector type machines* (National Academy of Sciences of Ukraine, Institute of geotechnical mechanics, Kyiv, 2001)
45. A. Bulat, A. Sokil, Non-stationary movement of a hydraulic mixture during condensation in technological equipment. Geotechnical mechanics 22, 3–7 (2000)
46. A. Shevchenko, N. Kolesnik, Crane vibration technologies in construction and safety. Lifting structures 14–15 (2003)
47. V. Poturaev, V. Franchuk, V. Naduty, *Vibration technology and technologies in energy-intensive industries* (NGA, 2002)
48. V. Naduty, E. Lapshin, L. Prokopishin, Experimental studies of the influence of vibration exciter parameters on the segregation process. Geotechnical mechanics 42, 136–142 (2003)
49. V. Naduty, E. Lapshin, Probabilistic processes of vibrational classification of mineral raw materials. Scientific thought 179 (2005)